Green Chemistry

PAPER

View Article Online
View Journal | View Issue

Cite this: *Green Chem.*, 2016, **18**, 1892

Identifying thermal phase transitions of lignin–solvent mixtures using electrochemical impedance spectroscopy†

Adam S. Klett, Jordan A. Gamble, Mark C. Thies* and Mark E. Roberts*

Received 29th September 2015,
Accepted 19th November 2015

DOI: 10.1039/c5gc02342d

www.rsc.org/greenchem

Lignin is unique among renewable biopolymers in having significant aromatic character, making it potentially attractive for a wide range of uses from coatings to carbon fibers. Recent research has shown that hot acetic acid (AcOH)–water mixtures can be used to recover "ultraclean" lignins of controlled molecular weight from Kraft lignins. A key feature of this discovery is the existence of a region of liquid–liquid equilibrium (LLE), with one phase being rich in the purified lignin and the other rich in solvent. Although visual methods can be used to determine the temperature at which solid lignin melts in the presence of AcOH–water mixtures to form LLE, the phase transition can be seen only at lower AcOH concentrations due to solvent opacity. Thus, an electrochemical impedance spectroscopy (EIS) technique was developed for measuring the phase-transition temperature of a softwood Kraft lignin in AcOH–water mixtures. In electrochemical cells, the resistance to double-layer charging (*i.e.*, polarization resistance R_p) is related to the concentration and mobility of free ions in the electrolyte, both of which are affected by the phases present. When the lignin–AcOH–water mixture was heated through the phase transition, R_P was found to be a strong function of temperature, with the maximum in R_P corresponding to the transition temperature obtained from visual observation. As the system is heated, acetate ions associate with the solid lignin, forming a liquefied, lignin-rich phase. This association increases the overall impedance of the system, as mobile acetate ions are stripped from the solvent phase and thus are no longer available to adsorb on the polarizing electrode surfaces. The maximum in R_P occurs once the new lignin-rich phase has completely formed, and no further association of the lignin polymer with AcOH is possible. Except at sub-ambient temperatures, the phase-transition temperature was a strong function of solvent composition, increasing linearly from 18 °C at 70/30 AcOH/water to 97 °C at 10/90 wt% AcOH/water.

1. Introduction

Lignin is one of the most abundant biopolymers, comprising about 30% of woody biomass; only cellulose is more commonplace. Furthermore, lignin is unique among renewable biopolymers in having significant aromatic content, as its molecular structure consists of interconnected and substituted phenylpropane units.[1] Thus, lignin is attractive for a wide range of uses for which renewable aliphatic polyesters such as polyglycolic acid (PGA) and polylactic acid (PLA) are less than suitable, including phenol–formaldehyde resins,[2,3] polyurethane foams,[4,5] specialty composites,[6,7] and carbon fibers.[8]

Because of the recalcitrant nature of lignin, many studies have been carried out on the extraction and recovery of lignin from biomass. For example, lignin recovery from wheat straw has been extensively studied, as it is an abundant agricultural waste,[9] as well as from prairie cordgrass, switchgrass, and corn stover.[10] For the extraction of lignin from wood, so-called organosolv processes, in which the wood is pulped with an organic solvent, have been extensively employed.[11,12] However, these processes have generally not been successful at producing lignin in a cost-competitive manner.

An alternative source of lignin is black liquor, a key by-product stream in the Kraft process, which is used to produce 95% of the wood pulp in the world today.[13] Approximately 50 million tons per year of lignin are available worldwide from black-liquor streams;[14] however, only about 0.2% of this lignin is recovered and sold commercially; the rest is burned in the recovery boiler of the pulp mill for its fuel value.[14] A significant issue that arises from the proposed use of this lignin for nonfuel applications is that black liquor contains ~20 wt%

Department of Chemical and Biomolecular Engineering, Clemson University, Clemson, SC, 29634-0909 USA. E-mail: mrober9@clemson.edu; Fax: +1-864-656-0784; Tel: +1-864-656-6307

†Electronic supplementary information (ESI) available. See DOI: 10.1039/c5gc02342d

metals on a dry basis,[15] primarily sodium added through the pulping chemicals sodium hydroxide and sodium sulfide. Several processes now exist for recovering low-ash lignin (containing 1–4% ash and <1% Na) from Kraft black liquor[16–18] (henceforth referred to as Kraft lignin), but many higher-value applications will require the recovered lignin to be "ultra-clean", that is, to contain less than 100 ppm metals.[19–21]

Recently, our team has discovered[22,23] that when Kraft lignin (a solid) is added to hot acetic acid–water mixtures, it dissolves to form two distinct liquid phases: (1) a solvent-rich liquid phase that preferentially extracts the metal salts along with the lower molecular weight (mol wt) lignin and (2) a lignin-rich liquid phase with a greatly reduced metals content that contains the higher mol wt lignin. Subsequent tests with our so-called ALPHA (Aqueous Lignin Purification with Hot Acids) process indicate that the sodium content of the recovered, higher mol wt lignin can be reduced to 25 ppm in two simple extraction steps with no additional washing.[22,23]

An important finding in the above work is that the temperature of the phase transition from solid to liquid lignin is a strong function of solvent composition. A visual method was used to detect this phase transition; however, for acetic acid/water ratios greater than 60/40 by mass, the solvent phase becomes dark and difficult to see through as it dissolves increasing amounts of lignin. Traditional methods for measuring phase transitions were attempted, but proved to be unsuccessful because of the unique nature of our system, namely, the presence of significant amounts of solvent (up to 90 wt%). For example, solvents prevented the use of differential scanning calorimetry (DSC), as the energy of the solid–liquid phase transition is negligible compared to the change in sensible heat of the solvent. Other techniques, such as thermal mechanical analysis (TMA) and dynamic mechanical analysis (DMA), were also eliminated from consideration, as property changes of the solvent phase (*e.g.*, thermal expansion or viscosity) render negligible any changes associated with the solid-to-liquid phase transition.

One technique that has been applied to characterizing phase transitions in polymer–solvent systems is electrochemical impedance spectroscopy (EIS). EIS is used to determine the resistive, capacitive, and inductive behavior of a complex system by measuring the current response to a small, oscillating AC potential applied to an electrochemical cell. Electrochemical processes, such as charge-transfer activation, double-layer capacitance, ohmic resistance and ion diffusion, occur over characteristic time scales and can be probed at different AC frequencies. By examining the electrochemical behavior over a wide range of frequencies (time scales), the impedance or resistance associated with these specific processes can be identified.

Previous work using EIS to characterize phase transitions in polymer-solvent systems, however, has been fairly limited. For example, we recently determined the effect of Li-ion concentration on the phase-transition temperature of a thermally responsive polymer in an ionic liquid,[24] and Alonso-García *et al.*[25] estimated the glass-transition temperature of polyelectrolyte brushes at solid–liquid interfaces *via* EIS. Impedance analysis has also been used to probe macroscopic property changes in other materials, such as the thermal transitions in hydrated layer-by-layer assemblies,[26] and to identify the critical temperature of superconductors.[27]

In this work, we used EIS to measure the solid–liquid phase-transition temperature of lignin over a wide range of acetic acid–water compositions. The polarization resistance, R_P, of these mixtures in a two-electrode cell was determined by fitting EIS data and was found to be a function of temperature. When the system was initially heated, R_P exhibited a maximum that correlated with the phase-transition temperature. This approach was used to identify the phase-transition temperature of various solvent compositions relevant to the ALPHA process.

2. Materials and methods

2.1. Materials

Glacial acetic acid (cat. no. MKV193-45) was supplied by Mallinckrodt. A softwood lignin was provided by Lignin Enterprises, LLC, which was produced *via* their sequential liquid–lignin recovery and purification process (SLRP™) from a softwood black liquor with a Kappa number of 25 and a solids content of 42 wt%. Deionized water was obtained from an in-house distillation apparatus followed by a water purification unit (Millipore™ Milli-Q Academic).

2.2. Sample preparation

Lignin–AcOH–water samples were prepared with solvent compositions ranging from 6/94 to 89/11 wt% water/AcOH, respectively. For mixtures with solvent compositions above 50% water, samples were prepared by mixing glacial acetic acid, distilled and deionized water, and lignin (sifted to mesh size 60) in 3-dram glass vials obtained from VWR (cat. no. 66011-100) at a solvent-to-lignin ratio of 1.5 ± 0.1 by mass. Approximately 0.25 g of this mixture were added to a button cell (MTI Corporation cat. no. EQ CR2025-CASE), followed by a stainless steel (SS) spacer and wave spring (MTI Corporation cat. no. EQ CR20-WS); the cell was subsequently crimped at a pressure of 1000 psig. Stainless steel strips were attached to the positive and negative terminals of the cell with an insulating rubber clip to serve as a connection between the cell and the potentiostat clips (Gamry Instruments Reference 600 Potentiostat/Galvanostat/ZRA). The SS strip on the positive side was connected to the working and sensing electrodes, and the SS strip on the negative side was connected to the counter and reference. The button cell assembly was then submerged into a silicon oil bath at 25 °C, and impedance measurements were taken as the oil was heated with a hotplate.

For mixtures with solvent compositions below 50% water, pre-weighed amounts of lignin and solvent were refrigerated separately at 4 °C for at least 12 hours before the experiments. The lignin and solvent were transferred to a box that was maintained at a temperature of around 0 °C while preparing the

cell. The lignin and solvent were combined, and the cell was assembled as described above in the cold box. The cell was then submerged into a silicone oil bath that had been pre-cooled to a temperature of 4 °C, and impedance measurements were taken as the oil was heated with a hotplate.

2.3. Electrochemical impedance spectroscopy analysis

Electrochemical impedance spectroscopy (EIS) measurements were performed on the button cells prepared as described above at a voltage of 0 V and an oscillating voltage amplitude of 10 mV rms, and the frequency was scanned from 10^5 Hz to 10^2 Hz. For the higher-temperature measurements, EIS data were taken every 2 °C from 25 to 110 °C. For the lower-temperature measurements, EIS data were taken every 1 °C from 4 to 55 °C. In both cases, the heating rate of the cell was 1 ± 0.2 °C min^{-1}. The temperature of the button cell was measured with a type K thermocouple attached to the outside of the cell and read with a Fluke 52 II Dual Input Digital Thermometer, which has a stated accuracy of ±0.3 °C. This thermocouple setup was checked against a calibrated secondary standard RTD (Burns engineering, model no. 18072-A-6-30-0-A/LT60); reported temperatures are accurate to within 0.5 °C.

3. Results and discussion

3.1. EIS measurements

EIS measurements were performed on lignin–AcOH–water mixtures over a range of temperatures and solvent compositions (*i.e.*, 6/94 to 89/11 wt% water/AcOH). The data was used to generate Nyquist plots, which show the real and imaginary components of the impedance. As an example, Fig. 1a presents Nyquist plots from 50 to 100 °C for lignin in a solvent mixture of 30/70 wt% AcOH/water. Data in the high-to-mid frequency range (*i.e.*, the semi-circles) were modeled as a simplified Randles cell (see Fig. 1a inset). In this model, the series resistance, R_S, can be found at the high-frequency (ω) intercept on the real axis. The value of the low-frequency intercept is the sum of the polarization resistance, R_P, and R_S. Because there is no charge transfer within the cell, the primary resistance at the electrode is R_P, which is represented by the intersection of the Nyquist plot with the real impedance axis at low frequency, where the imaginary part of the impedance is zero. As shown in Fig. 1a, R_S only slightly decreases with increasing temperature due to the increasing conductivity of the solvent. However, as shown in Fig. 1a and b, R_P exhibits a significant temperature dependence, initially increasing from 100 Ω to 6500 Ω as the cell is heated to 65 °C, and then gradually decreasing down to 900 Ω as the cell is further heated to 110 °C. Note in Fig. 1b that R_P exhibits a maximum with respect to temperature at 65 °C.

Interestingly, this maximum in R_P correlates with the visual solid–liquid phase transition observed in our previous work.[22] At room temperature, the solid lignin powder does not dissolve, but forms a muddy suspension in the AcOH–water mixtures. As these systems are gradually heated, R_P rapidly

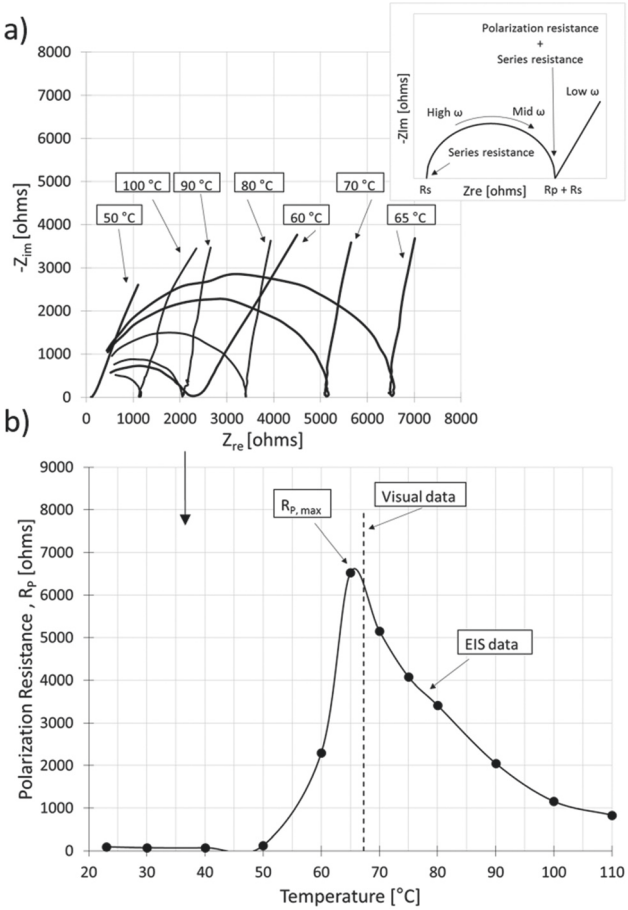

Fig. 1 (a) Nyquist plot series at different temperatures for the solvent composition of 30/70 wt% AcOH/water at a lignin to solvent ratio of 1.5. Inset illustrates how data in the mid-to-high frequency range were modeled as a simplified Randles cell. (b) Polarization resistance, R_P, *vs.* temperature for 30/70 wt% AcOH/water, with the maximum in R_P occurring at the phase transition from solid to liquid lignin in the presence of a solvent phase. EIS data are in good agreement with visual observation.

increases (*e.g.*, see Fig. 1b). This is probably due to the formation of lignin–AcO^- complexes in the newly formed lignin-rich liquid phase, which depletes the acetate ion concentration in the solvent. (Some water will also be present in these complexes, but in lesser amounts). Under this scenario, at the maximum in R_P (65 °C), the lignin has become completely solvated in the lignin-rich liquid, resulting in the formation of a liquid–liquid biphasic system. However, once the new lignin-rich phase has completely formed, further increases in temperature result in a steady decrease in R_P as the ionic conductivity of each liquid phase, the aqueous phase in particular, increases. Looking at the data in Fig. 1a, we infer that the decrease in conductivity is limited by the lower diffusivity of the lignin–AcO^- complexes in the lignin-rich liquid compared to free acetate ions and protons that exist in the aqueous phase at low temperature solution. In summary, because the phase transition involves the formation of such complexes,

which in turn affect the ionic content, EIS can be used to quantitatively identify the temperature at which the phase transition from solid lignin–liquid solvent to liquid lignin–liquid solvent occurs.

In Fig. 2a, the polarization resistance R_P is plotted as a function of temperature for various measured solvent compositions. Looking first at the effect of solvent composition, we see that at high water concentrations (87%) the maximum in R_P is relatively high (*i.e.*, 32 500 Ω), but as the solvent becomes more concentrated in acetic acid the maximum in R_P decreases. Increasing AcOH content leads to both higher solution conductivity and the availability of more acetate ions to complex with the lignin in the lignin-rich phase, both of which contribute to a lower R_P at the phase transition. The acetate ions in solution allow for electrode charging by assembling on the electrode interface to form a double layer upon polarization.[28] As the concentration of AcOH increases from zero, more ions are available in solution to move in response to the oscillating electric field; therefore, the impedance associated with electrode polarization decreases. However, below about 40% water the maximum in R_P monotonically increases with increasing AcOH content. The most likely explanation for this phenomenon is that below 40% water, the available AcOH has already complexed with the lignin, and any further increases in AcOH concentration come at the expense of decreasing water (and thus proton) content in solution, which decreases electrolyte conductivity.

The impedance characteristics of the lignin–AcOH–water system shown above are consistent with the conductivity behavior of neat AcOH–water solutions,[29] which also exhibit a similar trend of decreasing impedance (and increasing solvent conductivity) with increasing AcOH at higher water concentrations, followed by increasing impedance with increasing AcOH at lower water concentrations (see Fig. S.1 in the ESI†).

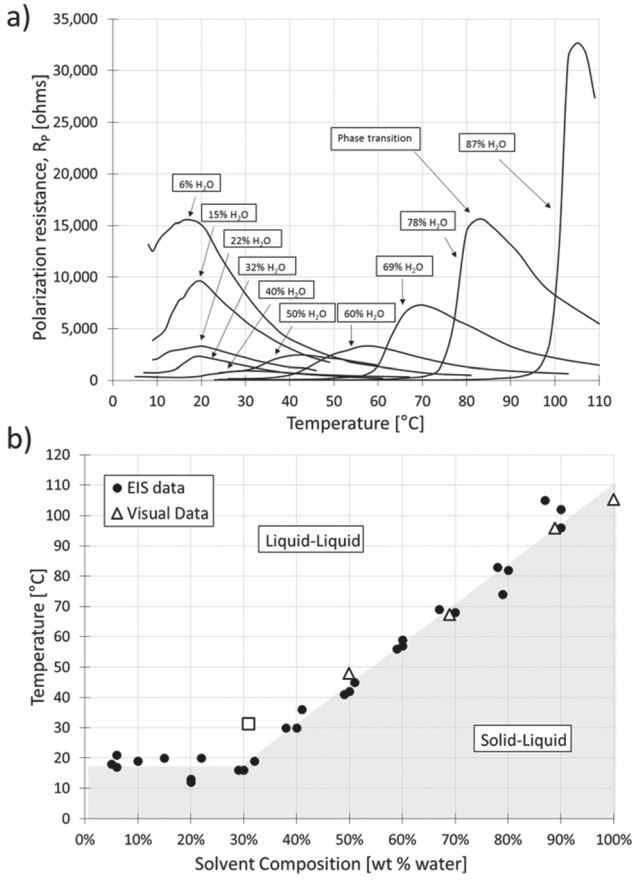

Fig. 2 (a) Polarization resistance, R_P, *vs.* temperature for lignin in selected AcOH/water solvent mixtures. For each profile, the maximum in R_P occurs at the phase-transition temperature. (b) Phase diagram for the lignin–AcOH–water system, showing phase-transition measurements at the phase boundary between the solid–liquid and liquid–liquid regions. The dark circles (●) represent EIS data, and white triangles (Δ) are from visual observation. The white square (□) is an example of the error in visual measurements at solvent compositions below 40 wt% water.

3.2. Phase diagram for lignin–acetic acid–water system

By plotting the temperatures at which R_P is a maximum in Fig. 2a as a function of solvent composition, a phase diagram for the lignin–AcOH–water system can be constructed. Such a diagram is given in Fig. 2b; however, here all measurements are shown – not just the more limited subset shown in Fig. 2a to avoid overcrowding. Shown are two distinct regions of phase behavior separated by the measured phase-transition boundary. Below the phase-transition temperatures, solid lignin is in equilibrium with a solvent-rich liquid phase (*i.e.*, solid–liquid equilibrium); above the phase-transition temperatures, a lignin-rich liquid phase is in equilibrium with a solvent-rich liquid phase (liquid–liquid equilibrium). Standard deviations in the reported temperatures and compositions were ±2.5 °C in temperature and ±0.5 wt% in composition (compositions are not more accurately known because of the uncertainty in the water content of the starting lignin). The effect of solvent-to-lignin ratio on the measured temperatures was investigated, and no effect between 0.7 and 1.9 was noted. At lower ratios, not enough solvent was present to make up the desired homogeneous mixture of toothpaste-like consistency; at higher ratios free solvent "puddles" would form, creating a heterogeneous system.

At solvent compositions where comparison is possible, phase-transition temperatures determined from EIS are in good agreement with those previously determined by visual observation. Visual measurements were performed by heating mixtures of acetic acid, water, and solid lignin particles in sealed glass vials placed in an oil bath, with the vial contents being continuously mixed with a magnetic stir bar. While increasing the temperature, the phase-transition temperature (within ±1 °C) was defined as the instant that swollen lignin particles coalesced to form a second liquid phase. Details are given elsewhere.[22] Recall that phase-transition temperatures could not be accurately determined visually for solvents containing less than 40% water because of the opacity of these solutions; an example of this disagreement is given in Fig. 2b,

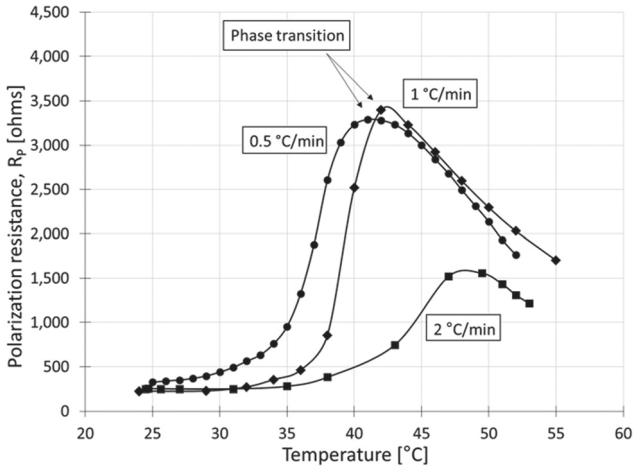

Fig. 3 Polarization resistance, R_P, *vs.* temperature for three different heating rates at a solvent composition of 50/50 wt% AcOH/water. For heating rates of 1 °C min^{-1} or less, the maximum in R_P occurs at the solid–liquid phase transition.

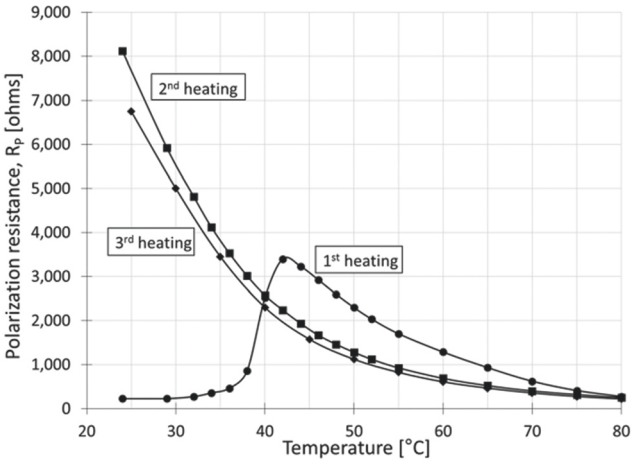

Fig. 4 Multiple heating scans of the same electrochemical cell loaded with solvent mixture (50/50 wt% AcOH/water) and lignin. For the first heating, R_P *vs.* temperature results show the solid–liquid phase transition. Re-heatings of the same cell show no such transition, as the acetic acid has already complexed with the lignin.

where the visually determined transition temperature for 30% water has been plotted as a square.

As shown in Fig. 2b, the phase-transition temperature boundary exhibits a linear correlation with water mass fraction down to 30% water. The plateau in the phase transition temperature observed at lower water concentrations may be attributable to the complete saturation of the lignin species with the acetate ions. Although the phase-transition temperature does not change in this low-water region, a significant increase in the system impedance is observed due to poor conductivity of the acetic acid solutions at these concentrations. Dimerization of the free acetic acid in a low-water environment[30] may be one cause of this increase in impedance.

The effect of heating rate on the measured phase-transition temperatures was investigated by varying the rate from 0.5 to 2 °C min^{-1}; the results are presented in Fig. 3. Clearly, a heating rate of 2 °C min^{-1} is too fast and introduces significant error between the maximum in R_P and the real phase-transition temperature. Kinetic limitations occur, both in the time required to heat the contents of the cell and in the time required for the mixture to achieve equilibrium at the new temperature. However, for heating rates of 0.5 and 1.0 °C min^{-1}, the measured phase-transition temperatures differed from each other by no more than a degree, indicating that heating rates within this range are suitable for determining the equilibrium phase-transition temperatures in our given setup.

Multiple sequential heating scans on lignin-solvent systems were used to investigate the electrochemical behavior after lignin had completely solvated in the AcOH–water mixture. Recall that when two phases were first formed by combining solid lignin and aqueous acetic acid with heating, the polarization resistance R_P reached a maximum at the phase-transition temperature and then monotonically decreased as the temperature was further increased. After cooling this two-phase mixture back to room temperature, a 2nd heating was performed. As shown in Fig. 4, R_P started at a dramatically higher value at ambient temperatures than when the two phases were first formed – but then monotonically decreased with increasing temperature down to values similar to those that were obtained during the initial formation of the two liquid phases. Third and subsequent heatings gave an R_P curve similar to that observed for the 2nd heating.

This behavior can be explained by considering the state of the sample for each of the heating steps. For the first heating, the system is a heterogeneous mixture of solid lignin and aqueous acetic acid. The low impedance (as measured by R_P) can be attributed to the free solvent (acetate and proton) ions present throughout the sample, as the lignin alone is not conductive and exhibits a high impedance. As the mixture is heated, R_P increases because of the association/complexing of the acetate ions with the lignin, which removes mobile ions from the solution. With further increases in temperature, the lignin polymer chains become even more mobile, and diffusion of these acetate ions into the polymer matrix takes place. This complexing of acetate ions with the lignin would be expected to increase the overall impedance of the system, as mobile ions are stripped from the solvent phase and thus are no longer available to adsorb on the polarizing electrode surfaces. This hypothesis is supported by the appearance of Nyquist semicircles (and thus R_P) as the temperature is further increased (see Fig. 1a). Once the mixture undergoes a phase transition to a two-phase system in liquid–liquid equilibrium, a decrease in R_P is observed with increasing temperature, as would be expected for two liquid phases.

But when this two-phase system is cooled back down to ambient, the acetate ions remain associated with the lignin polymer – even as the lignin once again solidifies. Clearly, the

acetate ions do not separate out to once again form an aqueous, acetic-acid phase of the original concentration! Once the two-phase system has cooled back down, the impedance measured before beginning the second heating is significantly higher. Then, as the sample is re-heated the measured R_P monotonically decreases, as no further complexation of the acetate ions with the lignin is possible (see Fig. 4).

Applications using lignin fractionated *via* the ALPHA process require accurate determination of polymer properties. For those interested, the physical properties of the lignin in each phase, such as molecular weight and salt content, are reported elsewhere.[22]

4. Conclusions

Electrochemical impedance spectroscopy has been shown to be a useful tool for determining the temperature at which a lignin polymer melts in the presence of acetic acid–water solutions. The polarization resistance, R_P, of electrochemical cells containing the above components was found to be a strong function of temperature, with the maximum in R_P corresponding to the phase-transition temperature associated with the "solid lignin–liquid solvent" to "liquid lignin–liquid solvent" equilibrium. A reliable, nonvisual method for determining the temperature at which a solvated, liquefied lignin polymer phase forms is important for the processing, fractionation, and purification of lignin streams using a safe solvent medium (*i.e.* AcOH–water).[22] The EIS technique described herein can potentially be extended to the characterization of other polymer–solvent systems; the best candidates will be those that contain solvent mixtures of components with significantly different ionic mobilities. Finally, in this work only the composition of the starting solvent mixture that was added to the starting solid lignin is known. If the fundamental chemistry that is at play in this complex, multicomponent system is to be elucidated, the solvent compositions in each of the two liquid phases that exist in equilibrium (*i.e.*, liquid lignin and liquid solvent) will need to be determined.

Acknowledgements

The authors would like to acknowledge the National Science Foundation (Award No. CBET-1403873) for financial support.

References

1 E. Adler, *Wood Sci. Technol.*, 1977, **11**, 169.
2 J. Domínguez, *et al.*, *Ind. Crops Prod.*, 2013, **42**, 308.
3 W. Qiao, *et al.*, *Ind. Eng. Chem.*, 2015, **21**, 1417.
4 P. Cinelli, I. Anguillesi and A. Lazzeri, *Eur. Polym. J.*, 2013, **49**, 1174.
5 J. Bernardini, *et al.*, *Eur. Polym. J.*, 2015, **64**, 147.
6 O. Gordobil, *et al.*, *Ind. Crops Prod.*, 2015, **72**, 46.
7 S. Hilburg, *et al.*, *Polymer*, 2014, **55**, 995.
8 M. Zhang and A. Ogale, *Carbon*, 2014, **69**, 626.
9 F. Zikeli, *et al.*, *Ind. Crops Prod.*, 2014, **61**, 249.
10 A. Cybulska, *et al.*, *Bioresour. Technol.*, 2012, **118**, 30.
11 A. Lindner and G. Wegener, *J. Wood Chem. Technol.*, 1988, **8**, 323.
12 E. Pye and J. Lora, *Tappi J.*, 1991, **74**, 113.
13 R. Patt, O. Korsdachia and R. Süttinger, *Pulp – Ullmann's Encyclopedia of Industrial Chemistry*, 2011.
14 R. Gosselink, *et al.*, *Ind. Crops Prod.*, 2004, **20**, 121.
15 J. Velez and M. Thies, *Bioresour. Technol.*, 2014, **148**, 586.
16 P. Tomani, *Cellul. Chem. Technol.*, 2010, **44**, 53.
17 L. Kouisni, *et al.*, *J. Sci. Technol. For. Prod. Processes*, 2012, **2**, 6.
18 M. Lake and J. Blackburn, Process for recovering lignin, *Int. Pat. Appl.*, PCT/US2010/049773, 2011.
19 A. L. Compere, W. L. Grifith, C. F. Leitten Jr. and J. T. Shaffer, *Low cost carbon fiber from renewable resources in International SAMPE Technical Conference Series: Advancing Affordable Materials Technology*, ed. A. Falcone, K. M. Nelson and R. Albers, Soc. Advancement Materials & Process Engineering, Seattle, WA, 2001, vol. 22, pp. 1306–1314.
20 G. Gellerstedt, E. Sjöholm and I. Brodin, *Open Agric. J.*, 2010, **3**, 119.
21 D. Baker and T. Rials, *J. Appl. Polym. Sci.*, 2013, **130**, 713.
22 A. Klett, P. Chappell and M. Thies, *Chem. Commun.*, 2015, **51**, 12855.
23 M. C. Thies, D. A. Bruce and A. S. Klett, Solvent and Recovery Process for Lignin, *US. Prov. Pat. Appl*, 62/081841, 2014.
24 J. Kelly, N. Degrood and M. Roberts, *Chem. Commun.*, 2015, **51**, 5448.
25 T. Alonso-García, *et al.*, *Anal. Chem.*, 2013, **85**, 6561.
26 C. Sung, K. Hearn and J. Lutkenhaus, *Soft Matter*, 2014, **10**, 6467.
27 A. Pinkowski, K. Jüttner and W. J. Lorenz, *J. Electroanal. Chem.*, 1990, **287**, 203.
28 A. J. Bard and L. R. Faulkner, *Electrochemical Methods: Fundamentals and Applications*, Wiley, New York, 2nd edn, 2001.
29 Gibson Research Corporation, https://www.grc.com/dev/ces/tns/Conductivity_v_Concentration.pdf, (accessed September 2015).
30 C. Tsonopoulos and J. M. Prausnitz, *Chem. Eng. J.*, 1970, **1**, 273.